Journal of Natural Sciences Research
ISSN 2224-3186 (Paper) ISSN 2225-0921 (Online)
Vol.3, No.15, 2013

Study of Anisotropy Superconductor using Time-Dependent Ginzburg-Landau Equation

Fuad Anwar[1,2*], Pekik Nurwantoro[1], Arief Hermanto[1]

1. Department of Physics, University of Gadjah Mada, Sekip Utara, Bulaksumur, Yogyakarta 55281, Indonesia
2. Department of Physics, University of Sebelas Maret, Jl. Ir. Sutami 36A, Kenthingan, Surakarta 57126, Indonesia

* E-mail of the corresponding author: fuada70@yahoo.com

Abstract

We have observed an anisotropy superconductor which was immersed in vacuum medium in presence of an applied magnetic field. The anisotropy properties of superconductor were related with two principal values of the effective mass of the Cooper pairs, namely m_c along the x-axis and m_{ab} in the yz-plane. Based on the time-dependent Ginzburg-Landau and ψU methods, the problem was solved and made to be the numerical simulation. From study using this numerical simulation, we can find that the anisotropy properties can make the critical field to be lower or higher.

Keywords: anisotropy, superconductor, time-dependent Ginzburg-Landau

1. Introduction

It is well known that the Time Dependent Ginzburg - Landau (TDGL) equations can be used to study the dynamics of superconductivity phenomenon (Tinkham 1996; Du 2005). These equations have nonlinear nature, so it will give results more completely to solve them numerically (Du 2005). One of the numerical solutions has been developed using the gauge invariant variables technique or to be called ψU method (Bolech *et al*. 1995; Gropp *et al*. 1996; Winiecki & Adams 2002). In the last decade, the solution of TDGL equations using ψU method has successfully been used to study the dynamics of superconductivity phenomenon in thin films (Barba *et al*. 2007; Barba *et al*. 2008; Barba-Ortega & Aguiar 2009; Barba-Ortega *et al*. 2010; Barba-Ortega *et al*. 2012; Barba-Ortega *et al*. 2013; Wisodo *et al*. 2013). However, these studies considered the superconductors having isotropy properties.

It is also well known that the high T_c superconductors have anisotropy properties (Tinkham, 1996). These superconductors are viewed as the stack of layers, each layer comprises the *ab* planes and the *c* axis is normal to them. The effective mass of the Cooper pairs is different when measured in the *ab* planes or along the *c* axis. The results in earlier papers show that the anisotropy properties have influence on superconductivity phenomenon (Hao & Hu 1996; Chapman & Richardson 1998; Achalere & Dey 2008).

In this paper, we study the dynamics of superconductivity phenomenon in an anisotropy superconductor using the TDGL equations and ψU methods. We describe the theoretical formalism and numerical method used for solving the problem in section 2. The results and their analysis are discussed in section 3. Finally, we conclude in section 4.

2. Numerical Methods

2.1 The Time-dependent Ginzburg-Landau Equations

The time-dependent Ginzburg-Landau (TDGL) equations are :

$$\frac{\hbar^2}{2m_s D}\left(\frac{\partial}{\partial t}+i\frac{e_s}{\hbar}\Phi(\mathbf{r},t)\right)\psi(\mathbf{r},t)=\frac{\hbar^2}{2m_s}\left(\nabla-i\frac{e_s}{\hbar}\mathbf{A}(\mathbf{r},t)\right)^2\psi(\mathbf{r},t)+|\alpha(T)|\psi(\mathbf{r},t)-\beta|\psi(\mathbf{r},t)|^2\psi(\mathbf{r},t) \quad (1)$$

$$\frac{1}{\mu_0}\nabla\times\left(\nabla\times\mathbf{A}(\mathbf{r},t)-\mu_0\mathbf{H}_{ext}(\mathbf{r},t)\right)$$
$$=\frac{\hbar e_s}{2m_s i}\left(\overline{\psi}(\mathbf{r},t)\nabla\psi(\mathbf{r},t)-\psi(\mathbf{r},t)\nabla\overline{\psi}(\mathbf{r},t)-\frac{2ie_s}{\hbar}|\psi(\mathbf{r},t)|^2\mathbf{A}(\mathbf{r},t)\right)+\sigma\left(-\nabla\Phi(\mathbf{r},t)-\frac{\partial\mathbf{A}(\mathbf{r},t)}{\partial t}\right) \quad (2)$$

where ψ is order parameter, **A** and $\mathbf{H_{ext}}$ denote the vector potential and an external magnetic field, e_s and m_s are the effective charge and the effective mass of the Cooper pairs, α dan β are phenomenological parameters, D is a phenomenological diffusion constant, Φ and σ are the electrical potential and conductivity (Bolech *et al*. 1995; Tinkham 1996; Gropp *et al*. 1996; Winiecki & Adams 2002).

In this study, we considered an anisotropic superconductor which is immersed in vacuum medium in presence of an applied magnetic field (The figure 1). Here, an anisotropic superconductor has layered structures, so it has two principal values of m_s, D and σ, namely : m_c, D_c and σ_c along the x-axis and m_{ab}, D_{ab} and σ_{ab} in the yz-plane. The applied magnetic field is assumed in the z-direction, time-dependent, and spatially uniform, so we have $\nabla\times\mathbf{H_{ext}}(t)=0$, $\mathbf{B}=B_z(x,y,t)\mathbf{z}$ and $\mathbf{A}=A_x(x,y,t)\mathbf{x}+A_y(x,y,t)\mathbf{y}$.

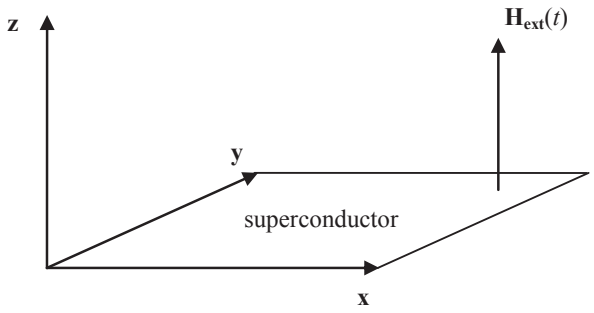

Figure. 1 An anisotropy superconductor in presence of an applied perpendicular uniform magnetic field

If we apply the previous assumption to the time-dependent Ginzburg-Landau, we can obtain :

$$\begin{aligned}
&\frac{\hbar^2}{2m_cD_c}\left(\frac{\partial}{\partial t}+i\frac{e_s}{\hbar}\Phi\right)\psi+\frac{\hbar^2}{2m_{ab}D_{ab}}\left(\frac{\partial}{\partial t}+i\frac{e_s}{\hbar}\Phi\right)\psi \\
&\quad=\frac{\hbar^2}{2m_c}\left(\frac{\partial}{\partial x}-i\frac{e_s}{\hbar}A_x\right)^2\psi+\frac{\hbar^2}{2m_c}\left(\frac{\partial}{\partial y}-i\frac{e_s}{\hbar}A_y\right)^2\psi+|\alpha|\psi-\beta|\psi|^2\psi \\
&\quad+\frac{\hbar^2}{2m_{ab}}\left(\frac{\partial}{\partial x}-i\frac{e_s}{\hbar}A_x\right)^2\psi+\frac{\hbar^2}{2m_{ab}}\left(\frac{\partial}{\partial y}-i\frac{e_s}{\hbar}A_y\right)^2\psi+|\alpha|\psi-\beta|\psi|^2\psi
\end{aligned} \tag{3}$$

$$\begin{aligned}
&\frac{1}{\mu_0}\frac{\partial}{\partial y}\left(\frac{\partial A_y}{\partial x}-\frac{\partial A_x}{\partial y}\right)\hat{x}-\frac{1}{\mu_0}\frac{\partial}{\partial x}\left(\frac{\partial A_y}{\partial x}-\frac{\partial A_x}{\partial y}\right)\hat{y} \\
&\quad=\frac{\hbar e_s}{2im_c}\left(\overline{\psi}\frac{\partial\psi}{\partial x}-\psi\frac{\partial\overline{\psi}}{\partial x}-\frac{2ie_s}{\hbar}|\psi|^2A_x\right)\hat{x}-\sigma_c\left(\frac{\partial\Phi}{\partial x}+\frac{\partial A_x}{\partial t}\right)\hat{x} \\
&\quad+\frac{\hbar e_s}{2im_{ab}}\left(\overline{\psi}\frac{\partial\psi}{\partial y}-\psi\frac{\partial\overline{\psi}}{\partial y}-\frac{2ie_s}{\hbar}|\psi|^2A_y\right)\hat{y}-\sigma_{ab}\left(\frac{\partial\Phi}{\partial y}+\frac{\partial A_y}{\partial t}\right)\hat{y}
\end{aligned} \tag{4}$$

Then, we scale ψ in $\psi_0=(|\alpha|/\beta)^{1/2}$, t in $\tau_c=\xi_c^2/D_c$, x and y in $\xi_c=(\hbar^2/2m_c|\alpha|)^{1/2}$, A_x and A_y in $A_{0x}=\mu_0Hc_{2c}\xi_c$, Φ in $\Phi_0=\xi_cA_{0x}/\tau_c$, σ_c and σ_{ab} in $\sigma_{0c}=1/(\mu_0\kappa_c^2D_c)$, and we choose $\Phi=0$, so we can rewrite equations (3) and (4) in the following form :

$$\left(\frac{1+\varepsilon_m^{\,2}\varepsilon_D^{\,2}}{\varepsilon_m^{\,2}\varepsilon_D^{\,2}}\right)\frac{\partial\psi}{\partial t}=\left(\frac{1+\varepsilon_m^{\,2}}{\varepsilon_m^{\,2}}\right)\left(\frac{\partial}{\partial x}-iA_x\right)^2\psi+\left(\frac{1+\varepsilon_m^{\,2}}{\varepsilon_m^{\,2}}\right)\left(\frac{\partial}{\partial y}-iA_y\right)^2\psi+2\left(1-|\psi|^2\right)\psi \tag{5}$$

$$\sigma_c\frac{\partial A_x}{\partial t}\hat{x}+\sigma_{ab}\frac{\partial A_y}{\partial t}\hat{y}=\frac{1}{2i}\left(\overline{\psi}\frac{\partial\psi}{\partial x}-\psi\frac{\partial\overline{\psi}}{\partial x}-2i|\psi|^2A_x\right)\hat{x}-\kappa_c^{\,2}\frac{\partial}{\partial y}\left(\frac{\partial A_y}{\partial x}-\frac{\partial A_x}{\partial y}\right)\hat{x}$$
$$+\frac{1}{2i\varepsilon_m^{\,2}}\left(\overline{\psi}\frac{\partial\psi}{\partial y}-\psi\frac{\partial\overline{\psi}}{\partial y}-2i|\psi|^2A_y\right)\hat{y}+\kappa_c^{\,2}\frac{\partial}{\partial x}\left(\frac{\partial A_y}{\partial x}-\frac{\partial A_x}{\partial y}\right)\hat{y} \tag{6}$$

In equations (5) and (6), we define :

$$\xi_c^{\,2}=\frac{\hbar^2}{2m_c|\alpha|}\quad\text{and}\quad\xi_{ab}^{\,2}=\frac{\hbar^2}{2m_{ab}|\alpha|} \tag{7a}$$

$$\lambda_c^{\,2}=\frac{m_c\beta}{\mu_0 e_s^{\,2}|\alpha|}\quad\text{and}\quad\lambda_{ab}^{\,2}=\frac{m_{ab}\beta}{\mu_0 e_s^{\,2}|\alpha|} \tag{7b}$$

$$\kappa_c^{\,2}=\frac{\lambda_c^{\,2}}{\xi_c^{\,2}}\quad\text{and}\quad\kappa_{ab}^{\,2}=\frac{\lambda_{ab}^{\,2}}{\xi_{ab}^{\,2}} \tag{7c}$$

$$Hc_{2c}=\sqrt{\frac{2}{\mu_0\beta}}|\alpha|\kappa_c\quad\text{and}\quad Hc_{2ab}=\sqrt{\frac{2}{\mu_0\beta}}|\alpha|\kappa_{ab} \tag{7d}$$

$$\varepsilon_m^{\,2}=\frac{m_{ab}}{m_c}=\frac{\xi_c^{\,2}}{\xi_{ab}^{\,2}}=\frac{\lambda_{ab}^{\,2}}{\lambda_c^{\,2}}=\frac{\kappa_{ab}}{\kappa_c}=\frac{Hc_{2ab}}{Hc_{2c}} \tag{7e}$$

$$\varepsilon_D^{\,2}=\frac{D_{ab}}{D_c} \tag{7f}$$

$$\varepsilon_\sigma^{\,2}=\frac{\sigma_{ab}}{\sigma_c} \tag{7g}$$

where ξ is the coherence length, λ is the penetration depth, and κ is the Ginzburg-Landau parameter.

The equations (5) and (6) can be solved by the ψU method (Bolech *et al*. 1995; Gropp *et al*. 1996; Winiecki & Adams 2002). In this method, the sample is divided into N_x x N_y cells, with mesh spacings Δ_x and Δy. At the cell, there are three fundamental unknowns, namely ψ, U^x and U^y. The $\psi_{i,j}$ is order parameter at position (x_i, y_j), with i = 1,2,…N_x+1 and j = 1,2,…,N_y+1. The U^x and U^y are the complex link variables and are related to **A** by :

(8a)

$$U_{i,j}^x=\exp\left(-i\int_{x_i}^{x_{i+1}}A_x(\xi,y_j)d\xi\right)\ \text{with}\ i=1,2,\ldots,N_x\ \text{and}\ j=1,2,\ldots,N_y+1 \tag{8b}$$

$$U_{i,j}^y=\exp\left(-i\int_{y_j}^{y_{j+1}}A_y(x_i,\eta)d\eta\right)\ \text{with}\ i=1,2,\ldots,N_x+1\ \text{and}\ j=1,2,\ldots,N_y$$

Using the ψU method and the Euler method and taking ε_D = 1, ε_σ = 1, σ_c=σ_{ab} = 1, the equations (5) and (6) can be derived in the following form :

$$\psi_{i,j}(t+\Delta t)=\psi_{i,j}(t)+\Delta t\left(\frac{U_{i,j}^x(t)\psi_{i+1,j}(t)-2\psi_{i,j}(t)+\overline{U}_{i-1,j}^x(t)\psi_{i-1,j}(t)}{\Delta x^2}\right)$$
$$+\Delta t\left(\frac{U_{i,j}^y(t)\psi_{i,j+1}(t)-2\psi_{i,j}(t)+\overline{U}_{i,j-1}^y(t)\psi_{i,j-1}(t)}{\Delta y^2}\right)$$
$$+2\Delta t\left(\frac{\varepsilon_m^{\,2}}{1+\varepsilon_m^{\,2}}\right)\left(1-|\psi_{i,j}(t)|^2\right)\psi_{i,j}(t) \tag{9}$$

$$U^x_{i,j}(t+\Delta t)\hat{x} = U^x_{i,j}(t)\hat{x} - i\Delta t U^x_{i,j}(t)\,\mathrm{Im}\left(U^x_{i,j}(t)\overline{\psi}_{i,j}(t)\psi_{i+1,j}(t)\right)\hat{x} - \kappa_c{}^2\frac{\Delta t}{\Delta y^2}U^x_{i,j}(t)\left(L_{i,j}(t)\overline{L}_{i,j-1}(t)-1\right)\hat{x} \quad (10)$$

$$U^y_{i,j}(t+\Delta t) = U^y_{i,j}(t) - \frac{i\Delta t}{\varepsilon_m{}^2}U^y_{i,j}(t)\,\mathrm{Im}\left(U^y_{i,j}(t)\overline{\psi}_{i,j}(t)\psi_{i,j+1}(t)\right)\hat{y} - \kappa_c{}^2\frac{\Delta t}{\Delta x^2}U^y_{i,j}(t)\left(\overline{L}_{i,j}(t)L_{i-1,j}(t)-1\right)\hat{y} \quad (11)$$

where,

$$L_{i,j} = U^y_{i+1,j}\overline{U}^y_{i,j}\overline{U}^x_{i,j+1}U^x_{i,j} \approx \exp\left(-i\Delta x\Delta y B_{z;i,j}\right) \quad (12)$$

2.2 The Boundary Conditions

In this study, we considered the superconductor is immersed in vacuum medium in presence of an applied magnetic field, so we have the boundary condition for ψ and **A**, namely :

$$\hat{\mathbf{n}}\cdot\left[-i\nabla - \frac{e_s}{\hbar}\mathbf{A}\right]\psi = 0 \quad (13)$$

$$B_{ext;z} = B_z = \frac{\partial A_y}{\partial x} - \frac{\partial A_x}{\partial y} \quad (14)$$

where *n* denotes the unit normal to the superconductor–vacuum interface.

If we apply the previous research assumptions and scale ψ in $\psi_0=(|\alpha|/\beta)^{1/2}$, x and y in $\xi_c=(\hbar^2/2m_c|\alpha|)^{1/2}$, A_x and A_y in $A_{0x}=\mu_0 Hc_{2c}\xi_c$, B_z and $B_{ext;z}$ in $\mu_0 Hc_{2c}$, H_z and $H_{ext;z}$ in Hc_{2c}, then we can use the ψU method and the Euler method to rewrite equations (13) and (14) in the following form :

at $i = 1$:

$$\psi_{1,j}(t) = U^x_{1,j}(t)\psi_{2,j}(t)$$
$$\psi_{N_x+1,j}(t) = \overline{U}^x_{N_x,j}(t)\psi_{N_x,j}(t) \quad (15a)$$

at $i = N_x+1$:

$$\psi_{i,1}(t) = U^y_{i,1}(t)\psi_{i,2}(t) \quad (15b)$$

at $j = 1$:

$$\psi_{i,N_y+1}(t) = \overline{U}^y_{i,N_y}(t)\psi_{i,N_y}(t) \quad (15c)$$

at $j = N_y+1$:

(15d)

and

at $i = 1$:

$$U^y_{1,j} \approx U^y_{2,j}\overline{U}^x_{1,j+1}U^x_{1,j}\overline{\exp\left(-i\Delta x\Delta y H_{ext;z}\right)}$$
$$U^y_{N_x+1,j} \approx U^y_{N_x,j}U^x_{N_x,j+1}\overline{U}^x_{N_x,j}\exp\left(-i\Delta x\Delta y H_{ext;z}\right) \quad (16a)$$

at $i = N_x+1$:

$$U^x_{i,1} \approx \overline{U}^y_{i+1,1}U^y_{i,1}U^x_{i,2}\exp\left(-i\Delta x\Delta y H_{ext;z}\right) \quad (16b)$$

at $j = 1$:

$$U^x_{i,N_y+1} \approx U^y_{i+1,N_y}\overline{U}^y_{i,N_y}U^x_{i,N_y}\overline{\exp\left(-i\Delta x\Delta y H_{ext;z}\right)} \quad (16c)$$

at $j = N_y+1$:

(16d)

2.3 The Numerical Simulation

We begin the numerical simulation with determining the value of N_x, N_y, Δx, Δy, Δt, κ_c and ε_m. We also assume the initial condition of superconductor as in a perfect Meissner state, so we have $H_{ext;z}=0$, $\psi_{i,j} = 1$, $U^x_{i,j}=1$ and $U^y_{i,j}=1$. Then, $H_{ext;z}$ is increased linearly with time and with small intervals of $\Delta H_{ext;z}$. When we have a new value of $H_{ext;z}$, we compute the new values of $\psi_{i,j}$, $U^x_{i,j}$ and $U^y_{i,j}$ using equations (9), (10), (11), (15) and (16).

Using this numerical simulation, we can also make magnetization curves. Magnetization can be calculated from :

$$\langle M_z\rangle = \langle B_z\rangle - H_{ext;z} \quad (17)$$

where M_z is scaled in Hc_{2c} and B_z is calculated by equation (12).

3. Results and Discussion

We try to run the numerical simulation with choosing five cases, namely : $\varepsilon_m = 1.0$, $\varepsilon_m = 0.5$, $\varepsilon_m = 0.8$, $\varepsilon_m = 1.3$, and $\varepsilon_m = 2.0$. For each case, the values of another input are the same, namely : $N_x = 32$, $N_y = 32$, Δ_x=0.5, Δ_y=0.5, $\Delta t = 0.010$, $\Delta H_{ext;z}$= 0.000001, and $\kappa_c = 2.0$. When $\varepsilon_m = 1.0$, it is the isotropy superconductor case and the others are the anisotropy superconductor cases.

In figure 2(a), we show the square modulus order parameter curve as a function of magnetic field $|\overline{\psi}|^2 - H_{ext}$ in the five cases. We can see in the figure, the $|\psi(x,y)|^2$ will completely vanish at the higher value of the applied field $H_{ext;z}$ when the value of ε_m increases. It means, by increasing ε_m the value of the surface nucleation field Hc_3 will be higher.

In figure 2(b), we show the magnetization curve as a function of magnetic field M-H_{ext} in the five cases. We can see, as increasing the applied field $H_{ext;z}$, the magnetization curve will decrease until the minimum value, then increase until the zero value. When the value of ε_m increases, we find that the minimum value will be located at the higher value of the applied field $H_{ext;z}$ if $\varepsilon_m \leq 1$ and at the lower value of the applied field $H_{ext;z}$ if $\varepsilon_m \geq 1$. We also find that the zero value will be located at the higher value of the applied field $H_{ext;z}$ when the value of ε_m increases. It means, by increasing ε_m, if $\varepsilon_m \leq 1$ the value of the lower critical field Hc_1 will be higher and if $\varepsilon_m \geq 1$ the value of Hc_1 will be lower. It also means, by increasing ε_m, the value of Hc_3 will be higher.

We show the distribution of the square modulus order parameter $|\psi(x,y)|^2$ on sample for five cases and for the several values of the applied field $H_{ext;z}$ in the figure 3-7. From these figures, we can see that in the low applied field $H_{ext;z}$, $|\psi(x,y)|^2$ has a high value. As increasing $H_{ext;z}$, the magnetic field will penetrate into sample to form vortex and $|\psi(x,y)|^2$ will decrease. When the value of ε_m increases, we find that $|\psi(x,y)|^2$ will vanish in the higher value of the applied field $H_{ext;z}$, the vortex is formed in the higher value of the applied field $H_{ext;z}$ if $\varepsilon_m \leq 1$ and in the lower value of the applied field $H_{ext;z}$ if $\varepsilon_m \geq 1$. Once again, these results mean that by increasing ε_m, the value of Hc_3 will be higher, if $\varepsilon_m \leq 1$ the value of Hc_1 will be higher and if $\varepsilon_m \geq 1$ the value of Hc_1 will be lower.

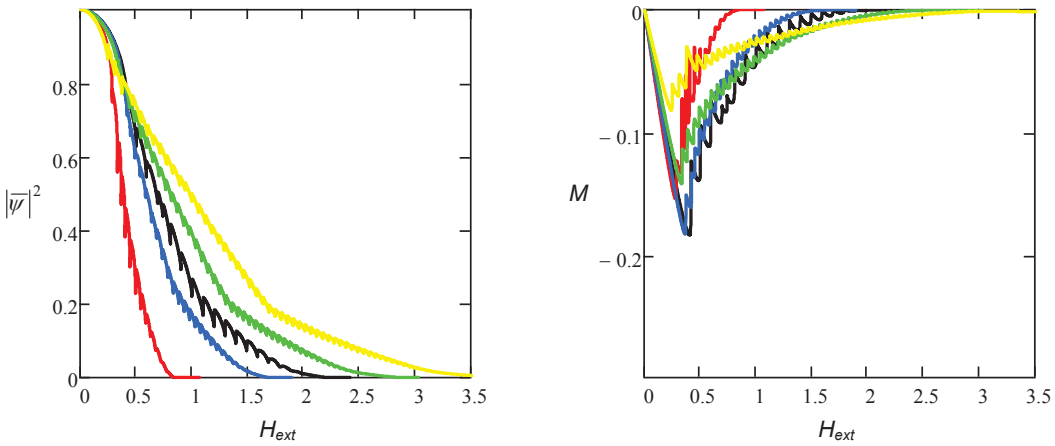

Figure 2. Plot of (a) $|\overline{\psi}|^2 - H_{ext}$ and (b) M-H_{ext} in the cases of :
— : $\varepsilon_m = 0.5$ — : $\varepsilon_m = 0.8$ — : $\varepsilon_m = 1.0$ — : $\varepsilon_m = 1.3$ — : $\varepsilon_m = 2.0$

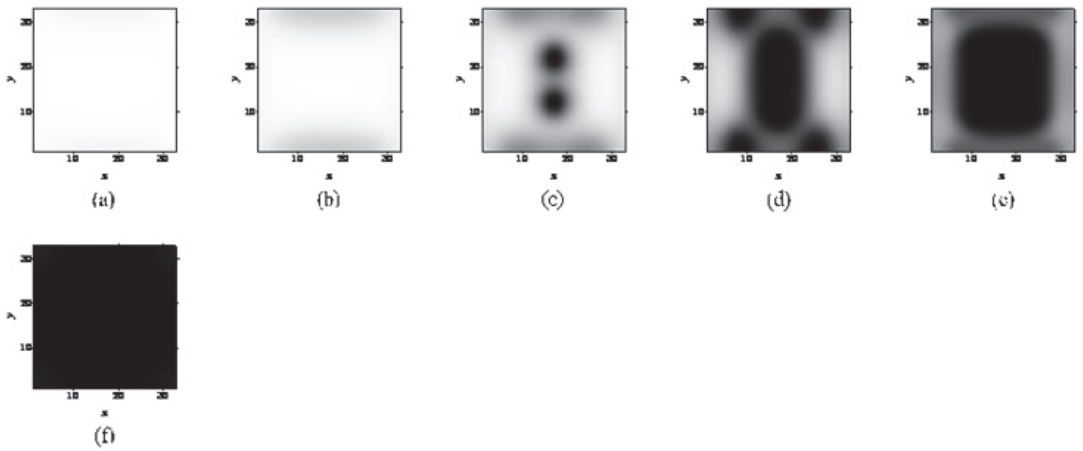

Figure 3. Plot of $|\psi(x,y)|^2$ in the case of ε_m=0.5 and (a)$H_{ext;z}$=0.10 (b)$H_{ext;z}$=0.20 (c)$H_{ext;z}$=0.30 (d)$H_{ext;z}$=0.40 (e)$H_{ext;z}$=0.50 (f)$H_{ext;z}$=0.80
The white and the black colours indicate $|\psi(x,y)|^2$=1 and $|\psi(x,y)|^2$=0.

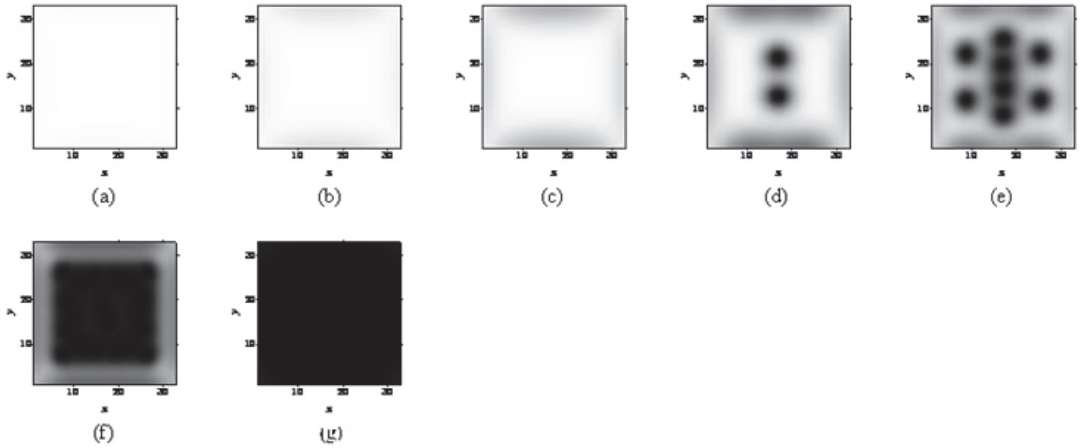

Figure 4. Plot of $|\psi(x,y)|^2$ in the case ε_m=0.8 and (a)$H_{ext;z}$=0.10 (b)$H_{ext;z}$=0.20 (c)$H_{ext;z}$=0.30 (d)$H_{ext;z}$=0.40 (e)$H_{ext;z}$=0.50 (f)$H_{ext;z}$=0.80 (g) $H_{ext;z}$=1.60
The white and the black colours indicate $|\psi(x,y)|^2$=1 and $|\psi(x,y)|^2$=0.

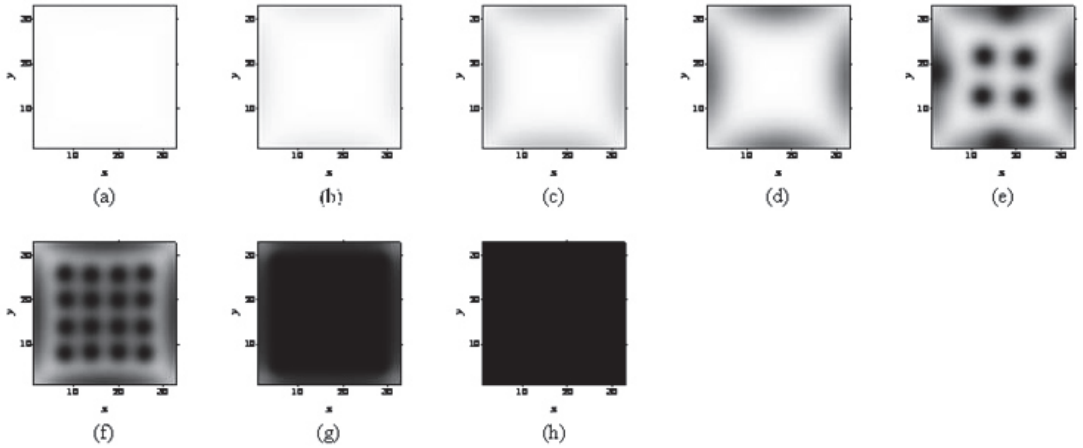

Figure 5. Plot of $|\psi(x,y)|^2$ in the case of ε_m=1.0 and (a)$H_{ext;z}$=0.10 (b)$H_{ext;z}$=0.20 (c)$H_{ext;z}$=0.30 (d)$H_{ext;z}$=0.40 (e)$H_{ext;z}$=0.50 (f)$H_{ext;z}$ =0.80 (g) $H_{ext;z}$=1.60 (h) $H_{ext;z}$=2.20.
The white and the black colours indicate $|\psi(x,y)|^2$=1 and $|\psi(x,y)|^2$=0.

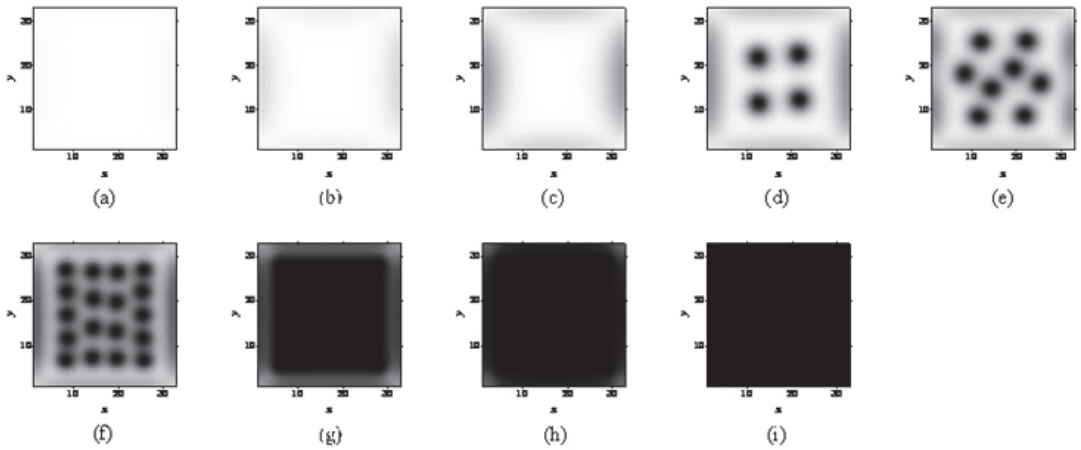

Figure 6. Plot of $|\psi(x,y)|^2$ in the case of ε_m=1.3 and (a)$H_{ext;z}$=0.10 (b)$H_{ext;z}$=0.20 (c)$H_{ext;z}$=0.30 (d)$H_{ext;z}$=0.40 (e)$H_{ext;z}$=0.50 (f)$H_{ext;z}$ =0.80 (g)$H_{ext;z}$=1.60 (h)$H_{ext;z}$=2.20 (i)$H_{ext;z}$=2.80.
The white and the black colours indicate $|\psi(x,y)|^2$=1 and $|\psi(x,y)|^2$=0.

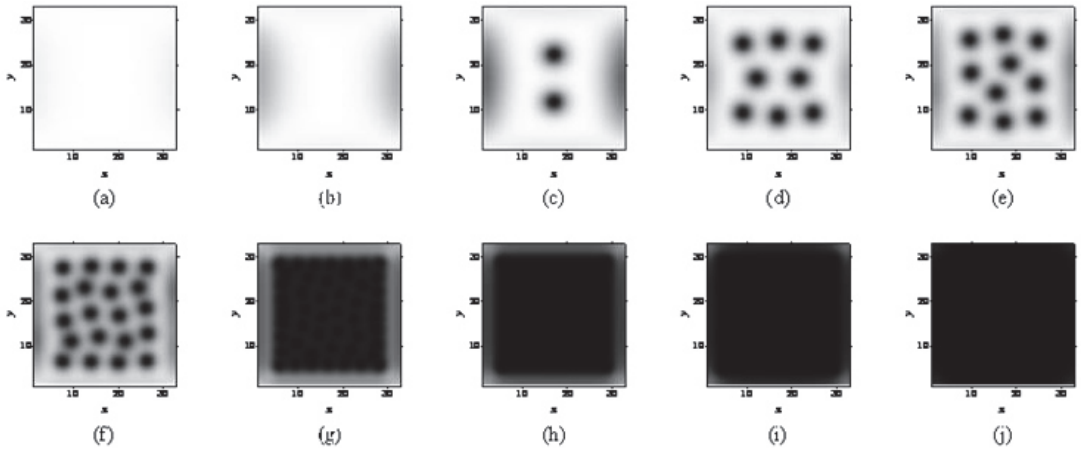

Figure 7. Plot of $|\psi(x,y)|^2$ in the case of ε_m=2.0 and (a)$H_{ext;z}$=0.10 (b)$H_{ext;z}$=0.20 (c)$H_{ext;z}$=0.30 (d)$H_{ext;z}$=0.40 (e)$H_{ext;z}$=0.50 (f)$H_{ext;z}$ =0.80 (g)$H_{ext;z}$=1.60 (h)$H_{ext;z}$=2.20 (i)$H_{ext;z}$=2.80 (j)$H_{ext;z}$=3.50
The white and the black colours indicate $|\psi(x,y)|^2$=1 and $|\psi(x,y)|^2$=0.

4. Conclusion

We have made a numerical solution of the Time Dependent Ginzburg - Landau (TDGL) equations for anisotropic superconductor using ψU methods. From this simulation, if we set κ_c in the fixed value and increase ε_m, we will obtain the value of Hc_3 will be higher and the value of Hc_1 will be higher if $\varepsilon_m \leq 1$and will be lower if $\varepsilon_m \geq 1$.

Acknowledgements

We thank to Direktorat Jenderal Pendidikan Tinggi (Ditjen Dikti)-Kementerian Pendidikan dan Kebudayaan (Kemdikbud)-Indonesia for the support of our research through BPPS scholarship.

References

Achalere, A. & Dey, B. (2008). Effect of *c*-axis Anisotropy on the Properties of High-T_c Superconductor Films of Finite Thickness. *Physica C*, 468, 2241-2249.

Barba, J. J., Cabral, L. R. E. & Aguiar, J. A. (2007). Vortex Arrays in Superconducting Cylinders. *Physica C*,

460-462, 1272-1273.

Barba, J. J., de Souza Silva, C. C., Cabral, L. R. E. & Aguiar, J. A. (2008). Flux Trapping and Paramagnetic Effects in Superconducting Thin Films : The Role of de Gennes Boundary Conditions. *Physica C*, 468, 718-721.

Barba-Ortega, J. & Aguiar, J. A. (2009). De Gennes Parameter Limit for The Occurrence of a Single Vortex in a Square Mesoscopic Superconductor. *Physica C*, 469, 754-755.

Barba-Ortega, J., Becerra, A. & Aguiar, J. A. (2010). Two Dimensional Vortex Structures in a Superconductor Slab at Low Temperatures. *Physica C*, 470, 225-230.

Barba-Ortega, J., Sardella, E., Aguiar, J. A. & Brandt, E. H. (2012). Vortex State in a Mesoscopic Flat Disk with Rough Surface. *Physica C*, 479, 49-52.

Barba-Ortega, J., Sardella, E. & Aguiar, J. A. (2013). Triangular Arrangement of Defects in a Mesoscopic Superconductor. *Physica C*, 485, 107-114.

Bolech, C., Buscaglia, G. C. & Lopez, A. (1995). Numerical Simulation of Vortex Arrays in Thin Superconducting Films, *Physical Review B*, 52, 22, R15719-R15722.

Chapman, S. J., & Richardson, G. (1998). Motion and Homogenization of Vortices in Anisotropic Type II Superconductors. *SIAM J. APPL. MATH.*, 58, 2, 587-606.

Du, Q. (2005). Numerical Approximations of The Ginzburg–Landau Models for Superconductivity. *J. Math. Phys*., 46, 095109-1 - 095109-22.

Gropp, W. D., Kaper, H. G., Leaf, G. K., Levine, D. M., Palumbo, M., & Vinokur, V. M. (1996). Numerical Simulation of Vortex Dynamics in Type-II Superconductors, *Journal of Computational Physics*, 123, 254-266.

Hao, Z. & Hu, C. R. (1996). Flux Motion in Anisotropic Type II Superconductors near H_{c2} with Arbitrary Vortex Orientation. *Jurnal of Law Temperature Physics*, 104, 3/4, 265-274.

Pascolati, M. C. V., Sardella, E. & Lisboa-Filho, P. N. (2010). Vortex Dynamics in Mesoscopic Superconducting Square of Variable Surface. *Physica C*, 470, 206-211.

Presotto, A., Sardella, E. & Zadorosny, R. (2013). Study of The Threshold Line between Macroscopic and Bulk Behaviors for Homogeneous Type II Superconductors. *Physica C*, 492, 75-79.

Tinkham, M. (1996). *Introduction to Superconductivity*. (2nd ed.). New York : McGraw-Hill, Inc.

Winiecki, T., & Adams, C. S. (2002). A Fast Semi-Implicit Finite Difference Method for The TDGL Equations. *Journal of Computational Physics*, 179, 127-139.

Wisodo, H., Nurwantoro, P., & Utomo, A. B. S. (2013). Voltage Curve for Annihilation Dynamics of A Vortex-Antivortex Pair in Mesoscopic Superconductor. *Journal of Natural Sciences Research*, 3, 9, 140-146.